

Received July 18, 2020, accepted July 22, 2020, date of publication July 27, 2020, date of current version August 7, 2020.

Digital Object Identifier 10.1109/ACCESS.2020.3012348

# Wideband Diplexer With Narrow Channel Spacing Using Hybrid Bandpass-Bandstop Structures

YAN-MEI XUE<sup>1</sup>, LIAN YANG<sup>1</sup>, JIN-XU XU<sup>1,2</sup>, XIAO-LAN ZHAO<sup>1</sup>,  
AND XIU YIN ZHANG<sup>1</sup>, (Senior Member, IEEE)

<sup>1</sup>School of Electronic and Information Engineering, South China University of Technology, Guangzhou 510641, China

<sup>2</sup>School of Electrical and Data Engineering, University of Technology Sydney, Ultimo, NSW 2007, Australia

Corresponding author: Jin-Xu Xu (xjinxu@126.com)

This work was supported by the National Natural Science Foundation of China under Grant 61725102 and Grant U1809203.

**ABSTRACT** In this paper, a wideband diplexer with narrow channel spacing is designed by using hybrid bandpass-bandstop structures. Two wideband bandpass structures are designed with the transmission zeros at the upper or lower passband edges to achieve high skirt selectivity. Two bandstop structures based on half-wavelength coupled lines are integrated to the two bandpass structures to introduce additional transmission zeros and thus the skirt selectivity is further improved. Accordingly, two channel filters with high skirt selectivity and high stopband rejection are designed to realize a wideband microstrip diplexer with very narrow channel spacing. For verification, a wideband diplexer operating at 1.71-2.17 GHz and 2.30-2.70 GHz is implemented, which covers multiple frequency bands for different mobile systems. The measured results show excellent performance of passband flatness, high in-band isolation of better than 35 dB and low minimum insertion losses of 0.46 and 0.50 dB for the two channels.

**INDEX TERMS** Diplexer, wide bandwidth, narrow channel spacing, hybrid bandpass-bandstop structure, transmission zero.

## I. INTRODUCTION

Diplexers are essential components in wireless systems, which have been widely developed using the waveguide/cavity, substrate integrated waveguide and printed circuit board (PCB) technologies [1]–[15]. With the development of wireless communication, the wireless spectrum is getting more crowded and the space between different frequency bands become narrower. This put forwards stringent requirements for the diplexers with a very narrow channel separation. The high- $Q$  waveguide/cavity [7]–[8], coaxial resonator [9] and organic liquid crystal polymer [10] are employed to realize diplexers with very narrow channel spacing. However, these diplexers are implemented with 3-D metallic structures, which suffer from heavy weight and large size, and thus are limited in some certain applications.

To solve this problem, microstrip diplexers on PCBs are also proposed for close channels [11]–[14]. For example, by adding an open-stub at the common input port, the diplexer is constructed using two ring filter with contiguous

passbands [11]. In [12], by using capacitance loaded square meander loop resonators, a close-channel diplexer is designed with compact size and wide stopband.

Apart from the narrow channel separation, wide channel bandwidths are also desired in order to cover multiple bands for different mobile systems, such as the DCS (1710-1880 MHz), PCS (1850-1990 MHz), UMTS (1920-2170 MHz), WiFi (2400-2480 MHz) and LTE (2300-2400 and 2570-2700 MHz). However, as the channel bandwidths increase, the frequency selectivity become worse. It is more difficult for wideband microstrip diplexers to realize high isolation between two contiguous channels. Thus, most of reported close-channel diplexers are designed with narrow bandwidths [11]–[14]. A good way for frequency selectivity improvement is to increase the filter orders whereas the insertion losses would be too high due to the  $Q$ -factor limitations of microstrip resonators. Until now, there are very few reported microstrip diplexers with both the narrow channel spacing and wide channel bandwidths.

In this paper, a wideband microstrip diplexer with narrow channel spacing is proposed. The two channel filters cover multiple frequency bands, including the DCS, PCS,

The associate editor coordinating the review of this manuscript and approving it for publication was Andrei Muller<sup>1</sup>.

UMTS, WiFi and LTE. Bandstop structures are integrated to the bandpass filter to generate transmission zeros at the passband edges to realize very high skirt selectivity and high rejection, which enable the realization of wideband diplexer with high isolation under narrow channel spacing applications. To demonstrate the proposed method, the diplexer is implemented. Simulated and measured results are presented. Comparison with other reported diplexers are given to show the advantages of the proposed circuit.

II. ANALYSIS OF THE DIPLEXER

Fig. 1 shows the structure of the proposed diplexer. The lower and upper channel filters are combined using a T-junction. The filter of each channel is designed into a hybrid bandpass-bandstop structure to realize high skirt selectivity and wide bandwidth. To construct the proposed diplexer, the lower and upper channel filters are analyzed as follows.

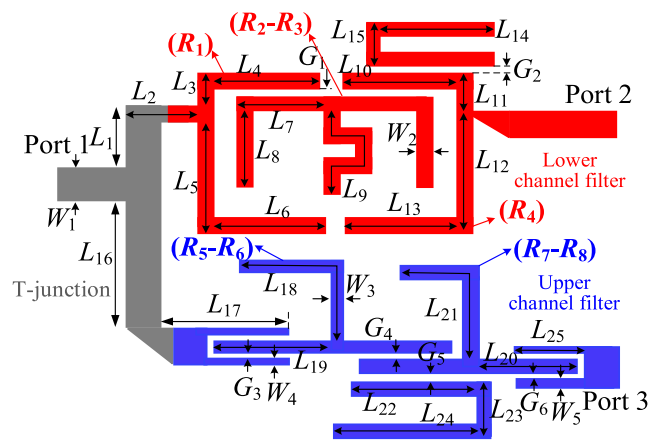


FIGURE 1. Schematic of the proposed diplexer.

A. LOWER CHANNEL FILTER

The structure of the lower channel filter is shown in Fig. 1 in red color, which contains the bandpass and bandstop sections. To construct this lower channel filter, the bandpass section is firstly designed with the structure shown in Fig. 2(a), which consists of two half-wavelength resonators (R1 and R4) and a dual-mode stub-loaded resonator (SLR) (R2-R3). Fig. 2(b) shows the topology of lower channel filter. To obtain the desired lower channel filter responses, the dual-mode SLR should be analyzed firstly, which is comprised of a main transmission line (TL) and an open stub loaded at the center. Resonant frequencies of the SLR can be analyzed using even- and odd-mode analysis methods in [16] as

$$f_{odd} = \frac{c}{2L_{m1}\sqrt{\epsilon_{eff}}} \tag{1}$$

$$f_{even} = \frac{c}{(L_{m1} + 2L_{m2})\sqrt{\epsilon_{eff}}} \tag{2}$$

where  $c$  is the speed of light in free space and  $\epsilon_{eff}$  is the effective dielectric constant. In Fig. 2(a), when the open stub of the SLR has quarter-wavelength electric length at a specific

frequency, the impedance at node A is equal to zero, namely, node A is short-circuited. The signal cannot be transmitted from P1 to P2, resulting in a transmission zero (TZ) whose location can be expressed as

$$f_{TZ} = \frac{c}{4L_{m2}\sqrt{\epsilon_{eff}}} \tag{3}$$

The  $f_{even}$  and  $f_{odd}$  are utilized to form the passband of lower channel filter. To realize better rejection at the upper channel frequency, the TZ should locate at the frequency higher than the passband of the lower channel filter. Thus,  $f_{TZ}$  should be larger than  $f_{even}$  and  $f_{odd}$ , namely,  $f_{TZ} > f_{odd}$  and  $f_{TZ} > f_{even}$ . From (1)-(3), it can be derived that  $L_{m2} < L_{m1} / 2$ . In this case, a BPF with a TZ located at the higher frequency of the passband can be realized. Fig. 2(c) shows the simulated results

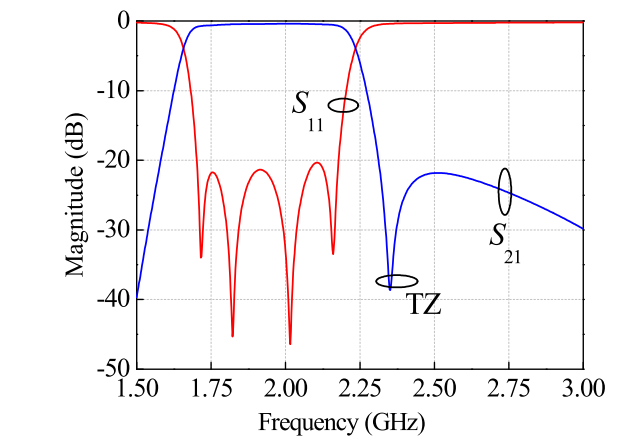
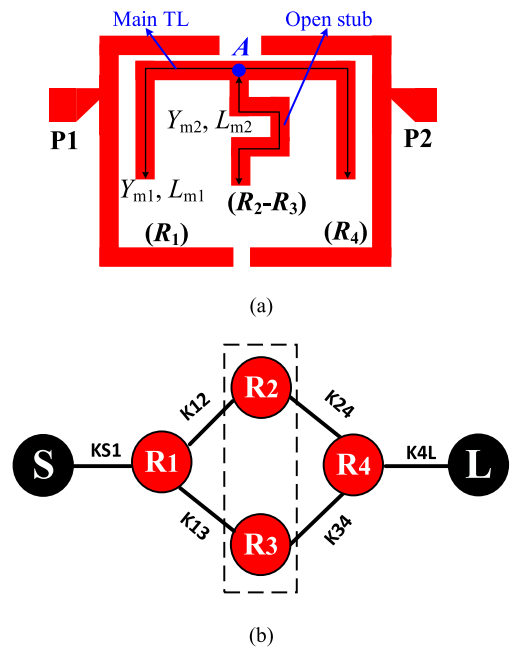


FIGURE 2. Bandpass section of the lower channel filter (a) Structure; (b) Coupling scheme; (c) Simulated results.

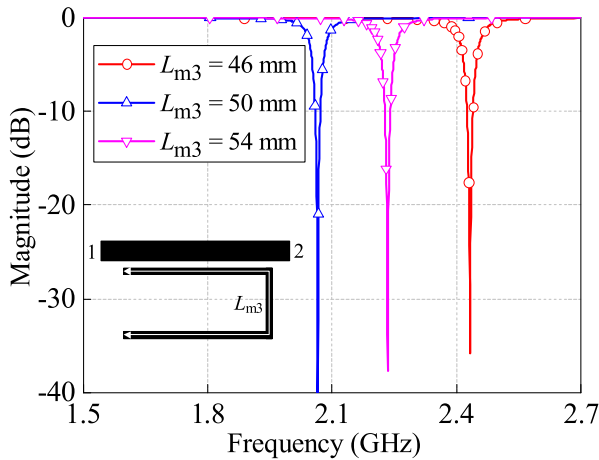


FIGURE 3. Simulated results of the bandstop structure.

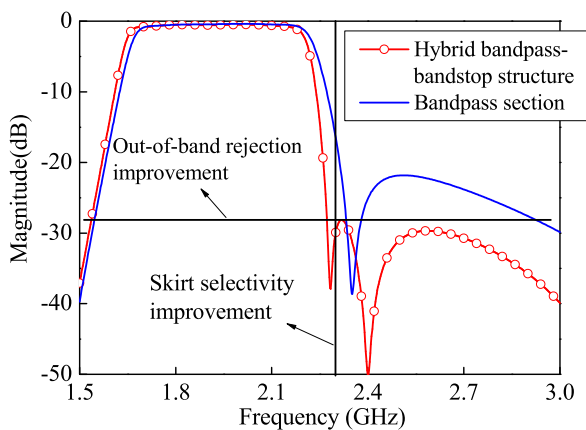


FIGURE 4. Simulated results of the BPF and hybrid bandpass-bandstop structure.

where a TZ is generated at the higher passband, resulting in high skirt selectivity.

Apart from the bandpass section, a bandstop structure comprised of a coupled half-wavelength transmission line (TL) is also introduced [17]. Fig. 3 shows its structure and the simulated results. As can be seen, a transmission zero can be generated and influenced by the length of the coupled TL ( $L_{m3}$ ).

In order to construct the lower channel filter with high out-of-band rejection and sharp roll-off-rate, the aforementioned bandpass and bandstop structures are combined together. Here, the half-wavelength TL can be coupled to any resonator or feeding line in the bandpass structure. For realizing an easy layout and a relatively compact size, the bandstop structure is coupled to R4 with the structure shown Fig. 1 (in red color). Fig. 4 shows the simulated results. It is seen that using the hybrid bandpass-bandstop structure not only enhances the skirt selectivity but also improves the out-of-band rejection.

### B. UPPER CHANNEL FILTER

Similar to the lower channel filter, an upper channel filter is also designed using the hybrid bandpass-bandstop structure, as shown in Fig. 1 (in blue color). Two dual-mode

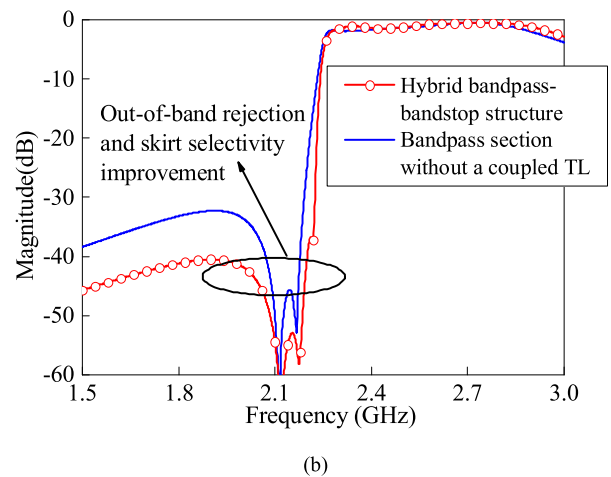
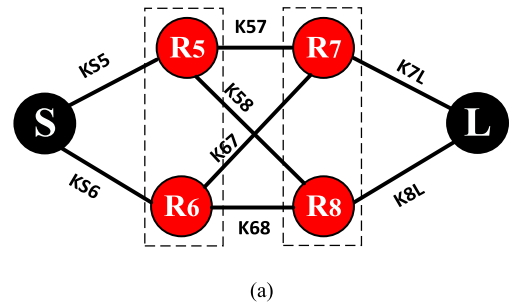


FIGURE 5. (a) Coupling scheme of the upper channel filter; (b) Simulated results of the upper channel filter.

stub-loaded resonators (R5-R6 and R7-R8) are utilized to form the passband, and the corresponding circuit topology is shown in Fig. 5(a). From the analysis in Part-A, It is known that two TZs can be generated by the two stub-loaded resonators and their locations are determined by the lengths of the stubs. Since the filter is used for the upper channel, the locations of the TZs should be lower than the passband. Thus, the length of each stub in the resonator should be larger than a half of the length of the main TL. A half-wavelength TL worked as the bandstop section is coupled to the R7-R8 for generating an additional TZ, which enhance the skirt selectivity. Fig. 5(b) shows the simulated results, where good filtering responses for the upper channel filter exhibits rejection underneath 40.5 dB. The skirt selectivity and out-of-band rejection are improved as compared to the structure without the bandstop section.

### III. EXPERIMENT

Based on the analysis in Section II, a diplexer is designed following the processes below. Firstly, based on the desired operation frequencies, two bandpass structures for the lower and higher channels using stub-loaded resonators are designed. Secondly, the bandstop structures are integrated to the two bandpass structures to realize the two channel filters. Thirdly, the two channel filters are combined using a T-junction with the structure shown in Fig. 1. Finally, fine tuning is required

to obtain good diplexer performance. The substrate is used with a dielectric constant of 2.55, a loss tangent of 0.0018 and a thickness of 1.524 mm. The dimensions are determined as follows (all in mm):  $L_1 = 11.25$ ,  $L_2 = 8.3$ ,  $L_3 = 4.3$ ,  $L_4 = 17$ ,  $L_5 = 26.4$ ,  $L_6 = 17.6$ ,  $L_7 = 14.3$ ,  $L_8 = 15.5$ ,  $L_9 = 24$ ,  $L_{10} = 16.8$ ,  $L_{11} = 5$ ,  $L_{12} = 24.5$ ,  $L_{13} = 15.8$ ,  $L_{14} = 22.7$ ,  $L_{15} = 3.7$ ,  $L_{16} = 31.6$ ,  $L_{17} = 16$ ,  $L_{18} = 26.6$ ,  $L_{19} = 17.7$ ,  $L_{20} = 17.9$ ,  $L_{21} = 26.6$ ,  $L_{22} = 20.6$ ,  $L_{23} = 8.5$ ,  $L_{24} = 20.6$ ,  $L_{25} = 12.4$ ,  $W_1 = 4.3$ ,  $W_2 = 0.5$ ,  $W_3 = 0.4$ ,  $W_4 = 0.4$ ,  $W_5 = 0.4$ ,  $G_1 = 0.53$ ,  $G_2 = 0.55$ ,  $G_3 = 0.3$ ,  $G_4 = 1$ ,  $G_5 = 1$ ,  $G_6 = 0.3$ . The circuit size is  $78 \times 68 \text{ mm}^2$  (or  $0.64 \times 0.56 \lambda_g^2$ , where  $\lambda_g$  is the guide wavelength at the frequency of lower passband edge 1.71 GHz). The photograph of the fabricated diplexer is shown in Fig. 6.

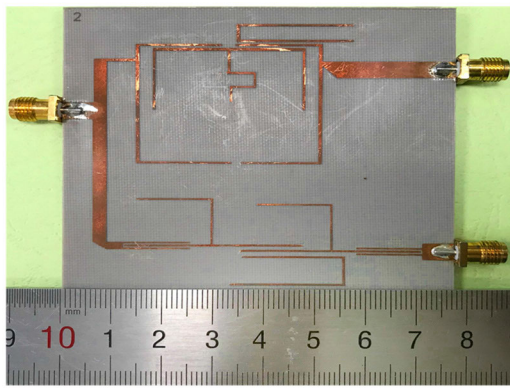
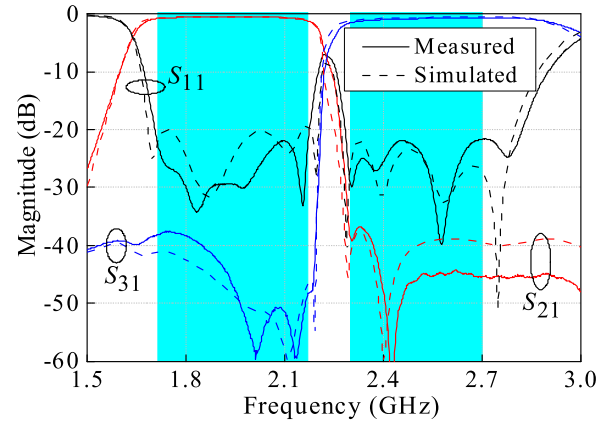


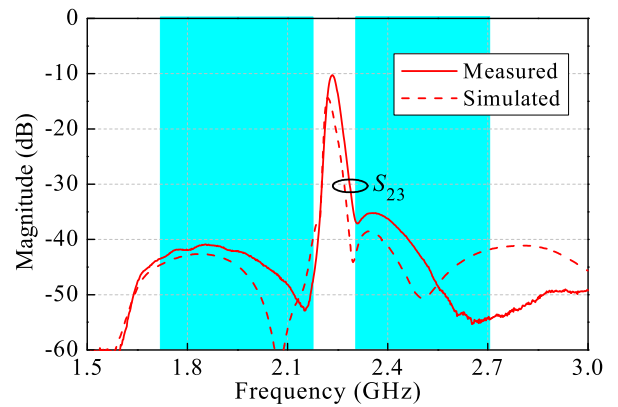
FIGURE 6. Photograph of the fabricated diplexer.

The simulation is carried out using the Zeland IE3D and the measurement is accomplished using Keysight E5071C network analyzer under a indoor temperature of 25 °C. Fig. 7 shows the simulated and measured results. The measured passbands are at 1.71-2.17 and 2.30-2.70 GHz with a narrow channel spacing of 130 MHz. The minimum insertion losses (ILs) of the two channels are 0.46 and 0.50 dB. The ILs within the whole passbands 1.71-2.17 and 2.30-2.70 GHz are smaller than 1.1 dB. The in-band return losses (RLs) of the two channels are both better than 20 dB, realizing good passband flatness. High out-of-band rejection of better than 37 dB and in-band isolation of better than 35 dB are achieved. The data as the temperature changes is not measured here due to our lab condition limitation. However, the proposed diplexer is fabricated using traditional PCB process. Thus, it is believed that the temperature behaviors of the presented diplexer are similar to those of other reported PCB circuits.

For evaluation of the radiation effect, the diplexer is enclosed in a conductive enclosure for measurement. Fig. 8 shows the photograph of the diplexer with the conductive enclosure. Fig. 9 shows the simulated and measured results. Within the passbands 1.71-2.17 GHz and 2.30-2.70 GHz, the measured insertion losses are less than 1.2dB. The measured return losses are better than 18 dB. For the upper-band rejection, it is around 10 dB. Accordingly, the proposed diplexer can realize good performance with or without the



(a)



(b)

FIGURE 7. Simulated and measured results (a)  $S_{11}$ ,  $S_{21}$  and  $S_{31}$ ; (b)  $S_{23}$ .

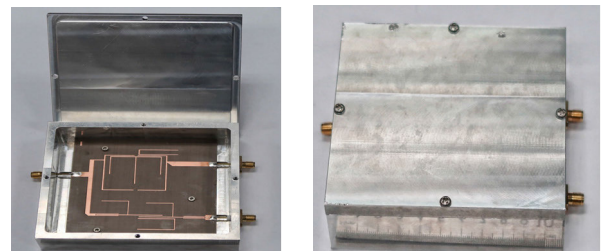


FIGURE 8. Photograph of the fabricated diplexer with a conductive enclosure.

conductive enclosure, which indicates that the radiation effect is negligible.

Table 1 shows the comparison with some reported diplexers. In [10], a contiguous diplexer is designed with wide operating frequency from DC to 100 GHz, whereas its complete assembly is a 3-D metallic waveguide structure which suffer from heavy weight. The proposed diplexer feature the fourth-order filtering responses while those in [11]–[14] have the second- or third-order responses. Thus, more resonators are used in our proposed design, which lead to a larger size. Here, the size of the proposed design can be optimized by folding the circuit. As compared to [11]–[15], the proposed

TABLE 1. Comparison with some report diplexers.

Ref.	Passband (GHz)	FBW (%)	Min. IL (dB)	Isolation (dB)	Return Loss (dB)	Filter orders	Circuit Size ( $\lambda_g^2$ )
[10]	DC-67 / 67-100	N.A.	N.A	N.A	10	N.A	N. A.
[11]	1.72-1.78 / 1.82-1.88	5 / 5	N.A	20	20	2	0.071
[12]	1.91-1.99 / 2.10-2.18	4.6 / 4.2	1.64 / 1.59	40	20	2	0.056
[13]	1.92-1.98 / 2.11-2.17	3.1 / 2.8	1.46 / 1.44	37	~ 16	2	0.213
[14]	1.91-1.99 / 2.11-2.18	4.1 / 3.74	1.2 / 1.5	35	~ 10	3	0.137
[15]	1.5-1.9 / 2.12-2.39 (3-dB passband)	23.2 / 11.8	N.A.	~ 38	~ 10	4	N.A.
This work (without conductive enclosure)	1.71-2.17 / 2.30 -2.70	30 / 27	0.46 / 0.50	35	20	4	0.414

N.A. means not available. IL. denotes insertion loss.

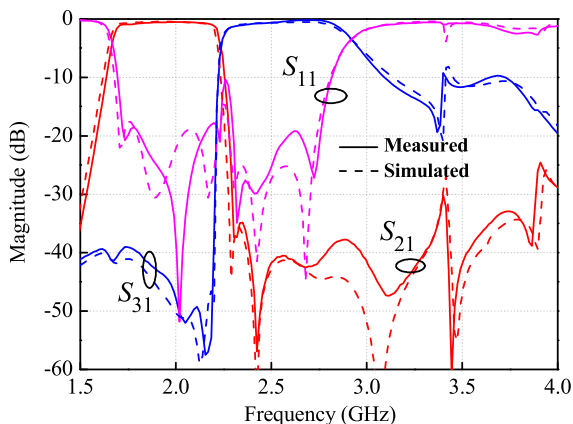


FIGURE 9. Simulated and measured results of the diplexer enclosed a conductive enclosure.

design exhibits the advantages of wide bandwidths (covering multiple bands for different systems from 1.71 to 2.70 GHz), flat passbands (the return losses are better than 20 dB in a wide frequency range), narrow channel spacing and low insertion losses (0.46 and 0.50 dB), which is attractive in base station applications.

#### IV. CONCLUSION

We have proposed a wideband microstrip diplexer with narrow channel spacing which covers multiple frequency bands for the DCS, PCS, UMTS, WiFi and LTE systems from 1.71 to 2.7 GHz. The bandpass-bandstop structures have been introduced to form the two channel filters. Multiple TZs have been generated, resulting in high out-of-band rejection and high skirt selectivity of each channel as well as high isolation between two channels. The circuit has been fabricated and measured. Comparison with other reported diplexers has been given to show the advantages of the proposed circuit.

#### REFERENCES

- [1] A. Fernandez-Prieto, A. Lujambio, J. Martel, F. Medina, F. Martin, and R. R. Boix, "Balanced-to-balanced microstrip diplexer based on magnetically coupled resonators," *IEEE Access*, vol. 6, pp. 18536–18547, 2018.
- [2] X. Guo, L. Zhu, and W. Wu, "Balanced diplexers based on inner-coupled dual-mode structures with intrinsic common-mode suppression," *IEEE Access*, vol. 5, pp. 26774–26782, 2017.
- [3] Y.-W. Chen, H.-W. Wu, C.-T. Chiu, and Y.-K. Su, "Design of new eight-channel diplexer for multiband wireless communication system," *IEEE Access*, vol. 6, pp. 49732–49739, 2018.
- [4] X. Guan, W. Liu, B. Ren, H. Liu, and P. Wen, "A novel design method for high isolated microstrip diplexers without extra matching circuit," *IEEE Access*, vol. 7, pp. 119681–119688, 2019.
- [5] K.-J. Song, Y.-D. Zhou, Y.-X. Chen, A. M. Iman, S. R. Patience, and Y. Fan, "High-isolation diplexer with high frequency selectivity using substrate integrate waveguide dual-mode resonator," *IEEE Access*, vol. 7, pp. 116683–116766, 2019.
- [6] J.-X. Xu and X. Y. Zhang, "Compact high-isolation LTCC diplexer using common stub-loaded resonator with controllable frequencies and bandwidths," *IEEE Trans. Microw. Theory Techn.*, vol. 65, no. 11, pp. 4636–4644, Nov. 2017.
- [7] L. Zhu, R. R. Mansour, and M. Yu, "Compact waveguide dual-band filters and diplexers," *IEEE Trans. Microw. Theory Techn.*, vol. 65, no. 5, pp. 1525–1533, May 2017.
- [8] B.-L. Zheng, S.-W. Wong, S.-F. Feng, L. Zhu, and Y. Yang, "Multi-mode bandpass cavity filters and diplexer with slot mixed-coupling structure," *IEEE Access*, vol. 6, pp. 16353–16362, 2018.
- [9] Z. Qi, X. Li, and J. Zeng, "Wideband diplexer design and optimization based on back-to-back structured common port," *IEEE Microw. Wireless Compon. Lett.*, vol. 28, no. 4, pp. 320–322, Apr. 2018.
- [10] I. Ashiq and A. P. S. Khanna, "Ultra broadband non-planar DC-67–100GHz contiguous diplexer implemented on organic liquid crystal polymer (LCP)," in *Proc. 46th Eur. Microw. Conf. (EuMC)*, Oct. 2016, pp. 1183–1186.
- [11] H.-S. Peng and Y.-C. Chiang, "Microstrip diplexer constructed with new types of dual-mode ring filters," *IEEE Microw. Wireless Compon. Lett.*, vol. 25, no. 1, pp. 7–9, Jan. 2015.
- [12] Q. Duan, K. Song, F. Chen, and Y. Fan, "Compact wide-stopband diplexer using dual mode resonators," *Electron. Lett.*, vol. 51, no. 14, pp. 1085–1087, Jul. 2015.
- [13] M.-L. Chuang and M.-T. Wu, "Microstrip diplexer design using common T-Shaped resonator," *IEEE Microw. Wireless Compon. Lett.*, vol. 21, no. 11, pp. 583–585, Nov. 2011.
- [14] X. Guan, F. Yang, H. Liu, and L. Zhu, "Compact and high-isolation diplexer using dual-mode stub-loaded resonators," *IEEE Microw. Wireless Compon. Lett.*, vol. 24, no. 6, pp. 385–387, Jun. 2014.

- [15] R. Gomez-Garcia, J.-M. Munoz-Ferreras, and M. Sanchez-Renedo, "Signal-interference stepped-impedance-line microstrip filters and application to duplexers," *IEEE Microw. Wireless Compon. Lett.*, vol. 21, no. 8, pp. 421–423, Aug. 2011.
- [16] X. Y. Zhang, J.-X. Chen, Q. Xue, and S.-M. Li, "Dual-band bandpass filters using stub-loaded resonators," *IEEE Microw. Wireless Compon. Lett.*, vol. 17, no. 8, pp. 583–585, Aug. 2007.
- [17] E. J. Naglich, A. C. Guyette, and S. Shin, "Microwave bandstop filters with minimum through-line length," in *IEEE MTT-S Int. Microw. Symp. Dig.*, May 2015, pp. 1–4.



**YAN-MEI XUE** was born in Changsha, Hunan, China, in 1994. She received the B.S. degree in communication engineering from Hunan Normal University, Changsha, in 2016. She is currently pursuing the Ph.D. degree in electronic and information engineering with the South China University of Technology, Guangzhou, China.

Her current research interests include microwave circuits, RF MEMS, and passive micromachined devices for communication applications.



**LIAN YANG** was born in Hefei, Anhui, China. She received the B.S. degree from Anhui University, Hefei, in 2017. She is currently pursuing the M.S. degree with the School of Electronic and Information Engineering, South China University of Technology, Guangzhou, China.

Her current research interest includes microwave circuits.



**JIN-XU XU** was born in Meizhou, Guangdong, China. He received the B.S. and Ph.D. degrees in electronic engineering from the South China University of Technology, Guangzhou, China, in 2015 and 2019, respectively.

From 2014 to 2015, he was a Research Assistant with the Shenzhen Key Laboratory of Millimeter-wave and Wideband Wireless Communications (MWWC), CityU Shenzhen Research Institute, Shenzhen, China. He is currently a Postdoctoral Research Associate with the Faculty of Engineering and Information Technology, University of Technology Sydney. He has authored or coauthored more than 40 internationally referred journal/conference papers. He is the co-inventor of nine granted Chinese patents and two granted U.S. patents. His current research interests include microwave circuits, MMIC, and millimeter-wave/terahertz integrated circuits and systems.

Dr. Xu was a recipient of the Best Student Paper Award presented at the IEEE MTT-S International Microwave Workshop Series on Advanced Materials and Processes for RF and THz Applications (IMWS-AMP), Chengdu, China, in 2016. He is a Reviewer of several internationally referred journals, including the IEEE TRANSACTIONS ON INDUSTRIAL ELECTRONICS and the IEEE TRANSACTIONS ON MICROWAVE THEORY AND TECHNIQUES.



**XIAO-LAN ZHAO** was born in Gansu, China. She received the M.S. and Ph.D. degrees in electronics engineering from the South China University of Technology, Guangzhou, China, in 2004 and 2013, respectively.

She is currently an Associate Professor with the School of Electronic and Information Engineering, South China University of Technology. Her current research interests include microwave circuits and low-temperature co-fired ceramic techniques.



**XIU YIN ZHANG** (Senior Member, IEEE) received the B.S. degree in communication engineering from the Chongqing University of Posts and Telecommunications, Chongqing, China, in 2001, the M.S. degree in electronic engineering from the South China University of Technology, Guangzhou, China, in 2006, and the Ph.D. degree in electronic engineering from City University of Hong Kong, Hong Kong, in 2009.

From 2001 to 2003, he was with ZTE Corporation, Shenzhen, China. From July 2006 to June 2007, he was a Research Assistant with the City University of Hong Kong. From September 2009 to February 2010, he was a Research Fellow with the City University of Hong Kong. He is currently a Full Professor and the Vice Dean of the School of Electronic and Information Engineering, South China University of Technology. He also serves as the Vice Director of the Guangdong Key Laboratory of Millimeter-Wave and Terahertz and the Vice Director of the Engineering Research Center for Short-Distance Wireless Communications and Network, Ministry of Education. He has authored or coauthored more than 140 internationally referred journal articles (including more than 90 IEEE TRANSACTIONS) and around 80 conference papers. His research interests include antennas and arrays, MMIC, microwave/terahertz circuits and sub-systems, and wireless communications.

Dr. Zhang is a fellow of the Institution of Engineering and Technology. He has served as a general chair/technical program committee (TPC) chair/member and a session organizer/chair for a number of conferences. He was a recipient of the National Science Foundation for Distinguished Young Scholars of China, the Leading Talent of Technological Innovation of Ten-Thousands Talents Program, the Young Scholar of the Changjiang Scholars Program of Chinese Ministry of Education, and the Scientific and Technological Award (First Honor) of Guangdong Province. He was a supervisor of several conference best paper award winners. He is an Associate Editor of IEEE ACCESS and the IEEE OPEN JOURNAL OF ANTENNAS AND PROPAGATION.

• • •